16th. Annual (International) Conference on Mechanical Engineering-ISME2008
May 14-16, 2008, Shahid Bahonar University of Kerman, Iran

# Dynamic Modeling of Chaotic Response of Bearing Systems due to Surface Defects

**Anoushiravan Farshidianfar** *Ferdowsi University of Mashhad* farshid@ferdowsi.um.ac.ir
**Ahmad Rafsanjani Abbasi** *Iran University of Science & Technology* rafsanjani@mecheng.iust.ac.ir
**Saeed Abbasion** *Iran University of Science & Technology* s.abbasion@mecheng.iust.ac.ir
**Hamid Moeenfard** *Sharif University of Technology* hamid.moeenfard@gmail.com

**Abstract**
In this paper an analytical model is proposed to study the nonlinear dynamic behavior of rolling element bearing systems including surface defects. The contact force of each rolling element described according to nonlinear Hertzian contact deformation and the effect of internal radial clearance has been taken into account. Mathematical expressions were derived for inner race, outer race and rolling element local defects. A modified Newmark time integration technique was used to solve the equations of motion numerically. The peak to peak frequency response of the system for each defect is obtained and the basic routes to periodic, quasi periodic and chaotic motions are determined. The current study provides a powerful tool for design and health monitoring of machine systems.
**Keywords:** Dynamic system modeling, rolling element bearing, local defect, linear stability, chaos

## Introduction

Rolling element bearings are one of the most widely used components in industrial applications. They have a great influence on the dynamic behavior of the rotating machines and act as a source of vibration and noise in these systems. There is a critical need to increase reliability and performance of rolling element bearings to prevent catastrophic failure of the machinery. However, the presence of a defect causes a significant increase in the vibration level. Bearing defects may be categorized as distributed or local. Distributed defects include surface roughness, waviness, misaligned races and off-size rolling elements [1]. They are usually caused by manufacturing error, improper installation or abrasive wear [2]. Local defects include cracks, pits and spalls on the rolling surfaces.

The early works on mechanical modeling of localized bearing defects was performed by McFadden and Smith [3]. Tandon and Choudhury [4] proposed an analytical model for predicting the vibration frequencies of rolling bearings and the amplitudes of significant frequency components due to a localized defect on outer race, inner race or on one of the rolling elements under radial and axial loads. Sopanen and Mikola [5] proposed a dynamic model for a deep groove ball bearing including localized and distributed defects, effect of internal radial clearance and unbalance excitation of the system.

Cao and Xiao [6] presented a dynamic model for double-row spherical roller bearing and studied various surface defects, including localized and distributed ones in their model. Recently, Tiwari et. al [7] and Harsha [8] investigated the stability of a rigid rotor supported by deep groove ball bearings and described the unstable ranges for different radial clearances but the stability of a rolling bearing rotor system containing local surface defects has not been studied before.

In this paper a mathematical method was developed based on the two-degree of freedom nonlinear model proposed by Fukata et. al [9]. In this model, the rolling elements are modeled as nonlinear springs according to Hertzian contact theory and the effect of loading zone has been taken into account. The surface defects including single point defects on raceways and rolling elements were introduced to this model with several mathematical expressions and the equations of motion were updated in each case. A modified Newmark time integration technique used to solve the equations of motion numerically [10]. The classical Floquet theory is applied to the proposed model to investigate the linear stability of the bearing system including local defects on raceways and rolling elements. Finally, the basic routes to chaos in rolling bearing systems are discussed in details.

## Defect Frequencies

There are some basic motions in rolling element bearings which demonstrate dynamics of the elements of rotating bearing and each has its specific frequency. These frequencies are illustrated in figure (1).

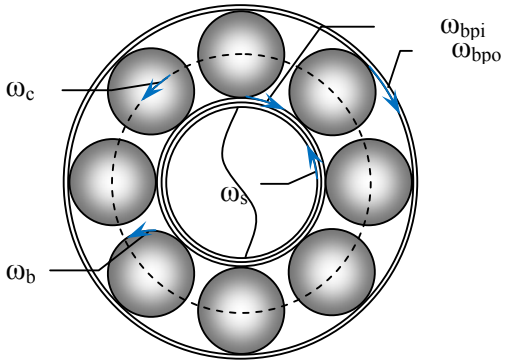


**Figure 1. Bearing defect frequencies**

They are cage frequency ($\omega_c$); ball passing inner race frequency ($\omega_{bpi}$), ball passing outer race frequency ($\omega_{bpo}$) and ball spin frequency ($\omega_b$). These frequencies are known as defect frequencies of rolling element bearings (see Appendix A for more details). Any defect in bearing elements, results in an increase of vibration energy at defect frequencies or combination of them [11].

**Bearing Vibration Model**

Consider the rolling element bearing is shown in figure (2). In this model which was developed by Fukata et. al. [9], the inner race of the bearing is assumed to have two degrees of freedom. The contact forces are summed over each of the rolling elements to give overall forces on the shaft and bearing housing. The overall contact deformation for jth rolling element, $\delta_j$, is given by

$$\delta_j = x\cos\theta_j + y\sin\theta_j - \gamma \tag{1}$$

Where $\gamma$ is the internal radial clearance. Neglecting the effect of rolling element inertia, the inner and outer race contact forces can be combined with an overall contact stiffness. The total restoring forces in x and y direction on the shaft and bearing housing is given by:

$$f_x = K\sum_{j=1}^{Z}\lambda_j\delta_j^{1.5}\cos\theta_j \qquad f_y = K\sum_{j=1}^{Z}\lambda_j\delta_j^{1.5}\sin\theta_j \tag{2}$$

where $\lambda_j$ is the loading zone parameter for $j$-th rolling element:

$$\lambda_j = \begin{cases} 1 & \delta_j > 0 \\ 0 & \delta_j \le 0 \end{cases} \tag{3}$$

In equation (2) $Z$ is the number of rolling elements and $K$ is the overall contact stiffness which is obtained from Hertzian deformation local to the contact zone. It depends on the geometry and material properties of the contacting surfaces [12]. $\theta_j$ is the angular position of jth rolling element which is given by:

$$\theta_j = \frac{2\pi(j-1)}{Z} + \omega_c t + \theta_0 \tag{4}$$

Where $\omega_c$ is the cage frequency and $\theta_0$ is the initial angular position of the first rolling element respect to x-axis. Now, the governing equations of motion can be obtained by applying the inertia, damping and restoring force to the inner race as following:

$$m\ddot{x} + c\dot{x} + f_x = W_x + f_u\cos\omega t \tag{5}$$

$$m\ddot{y} + c\dot{y} + f_y = W_y + f_u\sin\omega t \tag{6}$$

Where $m$ is the mass of inner race and the rotor supported by bearing and c is the equivalent viscous damping. $W_x$ and $W_y$ are the components of radial force acting on the rotor, $f_u$ is the unbalance force which is taken for balanced rotor as zero and $\omega$ is the shaft frequency. The governing equations of motion (5) and (6) are two coupled strongly nonlinear second order differential equations with parametric excitation.

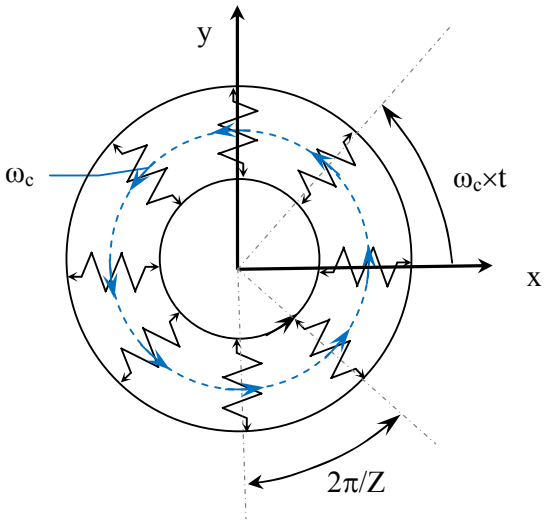


**Figure 2. Bearing Vibration Model**

**Surface Defect Modeling**

When a local defect such as pitting exists in one of the bearing components, a transient force occurs whenever another bearing component contacts the defective surface. A local fault produces an impulse having a repetition rate equal to the characteristic frequencies which can cause quite complex reactions within the bearing, for the purpose of modeling, the reaction can be approximated by a short term impulses. The impulses are modeled using the following operator:

$$\Lambda_d(\theta) = \begin{cases} 1 & |\theta| \le \theta_e \\ 0 & |\theta| > \theta_e \end{cases} \tag{7}$$

Where $\theta_e$ is the half of the desired length of the defect in tangential direction. The vibration produced by inner race defect can be modeled as a series of impulses repeating with the frequency of inner race contact angle:

$$I_d(t) = \sum_{j=1}^{Z}\Lambda_d(\mathrm{mod}(\theta_{ij}, 2\pi) - \frac{2\pi}{Z}(j-1) - \varphi_{id}) \tag{8}$$

For the case of localized defect on the outer race the vibration model is similar to that produced by an inner race defect. So the vibration generated due to outer race defect can be expressed as:

$$O_d(t) = \sum_{j=1}^{Z}\Lambda_d(\mathrm{mod}(\theta_{oj}, 2\pi) - \frac{2\pi}{Z}(j-1) - \varphi_{od}) \tag{9}$$

When there is a defect on the ball surface, the defect impacts two times per revolution of the ball about its own axis, one for inner ring and another for outer ring. So that the generated impulse is expressed as below:

$$R_{id}(t) = \Lambda_d(\mathrm{mod}(\theta_b, 2\pi) - \varphi_{bd}) \quad (10)$$

$$R_{od}(t) = \Lambda_d(\mathrm{mod}(\theta_b, 2\pi) - \pi - \varphi_{bd}) \quad (11)$$

And the total vibration generated due to rolling element defect can be expressed as

$$R_d(t) = R_{id}(t) + R_{od}(t) \quad (14)$$

**Linear Stability Analysis**

The classical Floquet Theory is applied to the system of nonlinear differential equations (5) and (6) to determine the linear stability of the bearing system. Consider

$$\dot{U}(t) = F(t, U(t), \sigma) \quad (15)$$

Where $\sigma$ is the bifurcation parameter and $U(t)$ and $F$ defined as

$$U(t) = \begin{bmatrix} x & y & \dot{x} & \dot{y} \end{bmatrix}^T \quad (16)$$

$$F = \begin{Bmatrix} \dot{x} \\ \dot{y} \\ -\frac{1}{m}\left( c\dot{x} + K\sum_{j=1}^{Z} \lambda_j \delta_j^{1.5} \cos\theta_j \right) \\ -\frac{1}{m}\left( c\dot{y} + K\sum_{j=1}^{Z} \lambda_j \delta_j^{1.5} \sin\theta_j \right) \end{Bmatrix} \quad (17)$$

The solution $\tilde{U}(t)$ of equation (15) is assumed to oscillate at the varying compliance frequency, so it has the period of $T = 1/\omega_{vc}$ where $\omega_{vc} = Z\omega_c$ is the varying compliance frequency, so that:

$$\tilde{U}(t) = \tilde{U}(t+T) \quad (18)$$

Substitution of the assumed solution (18) into equation (15) and introducing $u(t)$ as the perturbation of the periodic solution yeilds

$$\dot{\tilde{U}}(t) + \dot{u}(t) = F(t, \tilde{U}(t) + u(t), \alpha) \quad (19)$$

The Linearized perturbation equation can be determined by expanding $F$ as the Taylor series expansion and considering just the linear terms:

$$\dot{u}(t) = \mathbf{A}(t)u(t) \quad (20)$$

Where $\mathbf{A}(t) = \partial F / \partial \tilde{U}(t)$ which is a periodic function of period T. The elements of matrix **A** is given in Appendix B. By classical Floquet theory, any fundamental matrix $\mathbf{\Phi}$, which is defined as a non-singular matrix satisfying

$$\dot{\mathbf{\Phi}}(t) = \mathbf{A}(t)\mathbf{\Phi}(t) \quad (21)$$

Can be given as

$$\mathbf{\Phi}(t) = P(t)\exp(t\mathbf{R}) \quad (22)$$

$P(t)$ is a non-singular matrix of periodic functions with the same period T, and **R** is a constant matrix, whose eigenvalues are the characteristic exponents of dynamical system (20). If the fundamental matrix is normalized such that $\mathbf{\Phi}(t_0) = \mathbf{I}$, the monodromy matrix of the system (20) can be calculated as

$$\tilde{\mathbf{M}}_{\mathbf{T}} = \exp(T\mathbf{R}) = \mathbf{\Phi}(t_0)\mathbf{\Phi}(t_0 + T) \quad (23)$$

monodromy matrix $\tilde{\mathbf{M}}_{\mathbf{T}}$ does not depend on the initial time $t_0$ [26]. The eigenvalues of monodromy matrix give the Floquet multiplier of the system which can be used to determine the linear stability of the system [13].

**Results and Discussion**

The governing equations of motion introduced in previous section are solved numerically using the modified Newmark time integration technique [10] and the response of the system was obtained. The overall contact deformation of jth rolling element, $\delta_j$, was updated to include the effect of each defect as $\delta_j = x\cos\theta_j + y\sin\theta_j - (\gamma + I(t))$. As introduced in previous sections *I(t)* is the impulse function corresponding to each defect. The transient vibrations of the system were eliminated by introducing an appropriate damping to achieve the steady state response of the system. For a given mass 0.6 kg and $W_y$=6N in the present study, the damping coefficient was chosen to be 200Nm/s. As it was mentioned before when the bearing rotates the loaded zone will change as a function of time resulting in parametric excitations. In parametrically excited systems, it is always difficult to estimate the frequency content of the response in advance. This information is needed to determine the time step in the Newmark time integration method. Hence, in calculations the time step was chosen to be $\Delta t = 10^{-5}$. For fast convergence, the following initial conditions were applied to the system under investigation: initial displacements are ($x_0 = 1\mu m$, $y_0 = 1\mu m$) and the initial velocities set to be ($\dot{x}_0 = 0$, $\dot{y}_0 = 0$).

In the present study, the analysis applied to a 6205-2RSL JEM SKF deep groove ball bearing. The bearing specifications including bearing geometry, defect frequencies and size of each defect are listed in Table 1. This bearing used as motor shaft support at the drive end of a 2 hp, three-phase induction motor (left) (Reliance Electric 2HP IQPreAlert motor). There is also another bearing at the fan end of the motor which was not studied in this work. Single point faults were introduced to the test bearings using electro-discharge machining with fault diameters of 7 mils, (1 mil=0.001 inches). Digital data were collected at 12,000 samples per second. The test stand is shown in figure (3).

All data related to the bearing and the system under investigation belongs to Case Western Reverse Lab. and is with permission of Dr. Kenneth A. Loparo. More details about experimental setup are reported in [14].

**Figure 3. Experimental Setup**

In this step of study, the simulation results of a defective rolling element bearing containing single point defects on inner race, outer race and rolling elements are compared to experimental data. In order to reduce the effect of the noise on the gathered experimental data an orthogonal wavelet denoising was performed according to the procedure developed in [15]. After that, the frequency spectrum of the denoised signal can be produced using the conventional Fast Fourier Transform (FFT) to obtain frequency components in details.

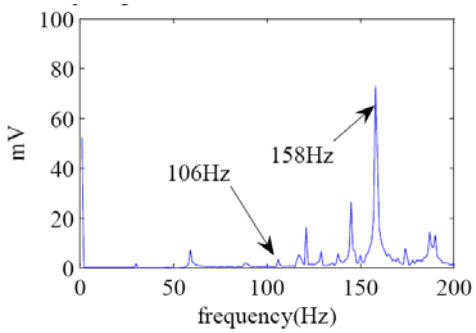


**Figure 4. Experimental FFT for inner race defect**

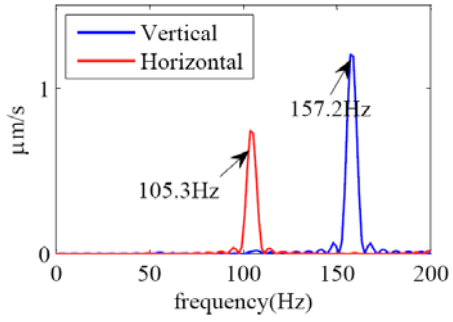


**Figure 5. FFT for inner race defect model**

As it can be seen from the figure (4) the response of the real system due to inner race defect contains two dominant peaks at 106Hz and 158Hz which can be recognized from the response obtained from the model as shown in figure (5). For other cases such comparison is available which was not mentioned here for brevity.

**Stability Analysis**

In this work, the response of rolling element bearings contain local surface defects on raceways and rolling elements is studied. The dynamic model developed in this study used for investigation of instability and the route to chaos in the dynamic response of the system as the operating speed of the system is changed. The steady state response of the rotor bearing system was obtained and the peak to peak response of the horizontal and vertical displacement plotted by numerical integration. The appearance of different regions of periodic, periodic doubling and chaotic behavior of the system for various local surface defects at different radial clearances would be discussed in this section.

Figure (6) shows the peak to peak displacement response of a bearing system without any defect in horizontal and vertical directions. Now, the peak to peak displacement response of a bearing system with single point defect on inner race, outer race and rolling elements would be studied. The peak to peak response is plotted in horizontal and vertical directions. Considering the response over a large range of rotational speed, 500-5000 rpm, the motion may be simply categorized at any particular speed to various regions.

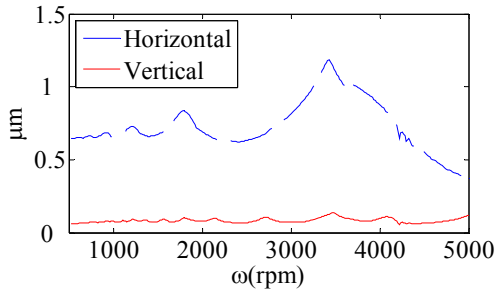


**Figure 6. Response for Normal Bearing**

Figure (7) shows the response of a bearing system with single point defect on inner raceway with small radial clearance (5μm). The response of the system indicates the characteristics of a softening nonlinear system. It contains peaks accompanied by jump phenomena and transition stages. The motion is completely chaotic at low speeds up to 1000rpm but as the speed increases the stability returns to the system and the transition stages grow off. In these regions, i. e. 1450-1600rpm or 2300-3200rpm, the motions is quasi-periodic because of the net structure of the phase trajectories and there are period doubling bifurcations. At the end of each stage, i. e. 1650rpm or 3290rpm, the fold bifurcation take places and the jump in the response of the system occurs. Because of this bifurcation, the motion leads to instability after which chaos suddenly appears. As speed increases the stability returns in next transition stage through period doubling bifurcations. At high shaft speeds the time responses show beating and chaotic behavior.

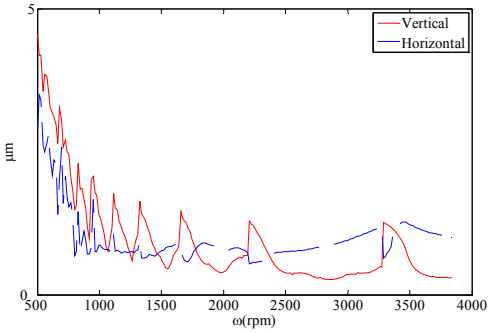


**Figure 7. Response for Inner Race Defect**

In the case of an outer race defect, the response is shown in figure (8). Here also the stiffness softening characteristic of the system is quite apparent. It can be seen that response curve contains jump phenomena and transition stages. It was also observed that except around the jump regions the response curve is similar to those obtained from a normal bearing. The most important route to unstable periodic solutions along transition stages is period doubling. The jump phenomena occur through fold bifurcation in an interior crisis route to chaos. The sudden increase in the size of a chaotic attractor occurs while the chaotic attractor collides with periodic orbits in the interior of its basin. The interior crisis route to chaos induces intermittency in the system which leads to a permanent jump between two chaotic attractors. These are regions of multivalued solutions which it is difficult to find all periodic solutions by numerical integrations. The eigenvalues of the monodromy matrix cross from +1. Another pattern of transition response is periodic in waveform which occurs almost at high operational speeds

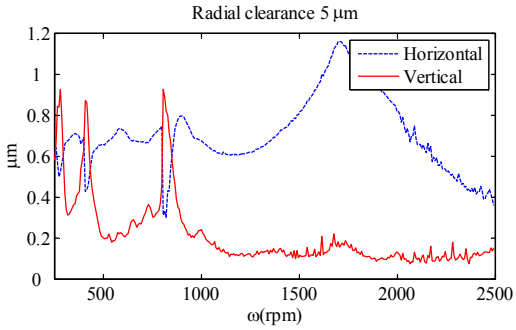


**Figure 8. Response for Outer Race Defect**

Now, the stability and the nature of the solution in presence of a single point defect on one of the rolling elements would be discussed. Figure (9) shows the response curve for small value of radial clearance γ=5µm. As it can be seen the response here also contains successive jump phenomena and transition stages

It can be seen that the response is similar to what was detected in the case of inner race defect at this clearance but the peaks in which jump occurs shifted to left in this figure. The basic route to chaos in small clearances is interior crisis. The nature of the motion in transition stages is quasi periodic. In the regions far from jump peaks, the stability increases as speed increases.

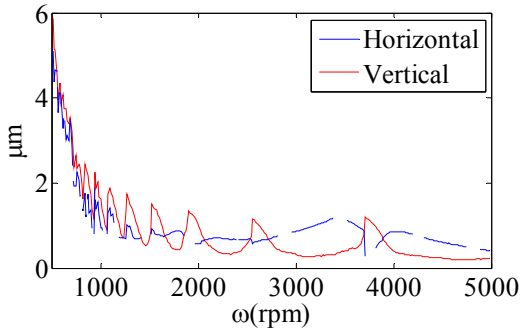


**Figure 9. Response for Rolling Element Defect**

**Conclusion**

In this paper the effect of local surface defects on the stability and the dynamic response of a rolling element bearing rotor system were investigated using an analytical model. The response of the bearing system was compared with those obtained from experiments. The accordance of the frequency components obtained from the mathematical model with those appeared in the frequency spectrum of the experimental data verifies the validity of the proposed model. It was investigated that the defect frequencies are slightly different from calculated values as a consequence of slipping and skidding in the rolling element bearings.

The linear stability analysis of the system indicates the existence of stable and unstable regimes in the response of the system. This analysis shows that in most range of shaft speeds, the system is not depended on initial conditions but strongly affected by the surface defects. According to the results of the current simulation, the important routes to chaotic motion for small radial clearance can be categorized as following:

The basic route to chaos is interior crisis and jump phenomena though fold bifurcations. There are transition stages in which the period doubling is the usual route to instability and quasi periodic solutions. The nonlinearity bends the frequency response to the left which indicates softening characteristic of the system. The bending of the frequency response leads to multivalued amplitudes and hence the jump phenomena. The location of defect at small clearance affects the frequency at which the jump occurs. For outer race defect the peaks occurs at low shaft speeds while in the case of inner race and rolling element defect the response contain several peaks as speed increases. The peak frequencies are different in each case.

The current study gives designers a powerful tool for prediction of the trends of instability in rolling element bearing rotor systems in the presence of local surface defects. The proposed model can be used for design, predictive maintenance and also condition monitoring of machines.

**Acknowledgment**

The authors would like to thank Dr. Kenneth A. Loparo for his excellent technical help for the experimental aspects of the work.

**References**

[1] Tallian TE, Gustafsson OG. Progress in rolling bearing vibration research and control. ASLE Trans 1965; 8(3):195–207.

[2] Sunnersjo CS. Rolling bearing vibrations - geometrical imperfections and wear. J Sound Vib 1985; 98(4):455–74.

[3] McFadden PD, Smith JD. Model for the vibration produced by a single point defect in a rolling element bearing. J Sound Vibr 1984;96(1):69–82.

[4] Tandon N, Choudhury A. An analytical model for the prediction of the vibration response of rolling element bearings due to a localized defect. J Sound Vibr 1997;205(3):275–92.

[5] Sopanen J, Mikola A. Dynamic model of a deep-groove ball bearing including localized and distributed defects. Part 1: theory. P I Mech Eng K-J MBD 2003; 217:201–211.

[6] Cao M, Xiao A. A comprehensive dynamic model of double-row spherical roller bearing-Model development and case studies on surface defects, preloads, and radial clearance. J Mech Syst Signal Pr 2007; in press.

[7] Tiwari M, Gupta K, Prakash O. Effect of radial internal clearance of a ball bearing on the dynamics of a balanced horizontal rotor. J Sound Vib 2000; 238(5):723–756.

[8] Harsha SP. Nonlinear dynamic analysis of an unbalanced rotor supported by roller bearing. Chaos Soliton Fract 2005; 26: 47-66

[9] Courrech J, Eshleman RL in: Harris CM (Ed.). Condition monitoring of machinery, Harris' Shock and Vibration Handbook. 5th Edition, New York: McGraw-Hill; 2002.

[9] Fukata S, Gad EH, Kondou T, Ayabe T, Tamura H. On the radial vibrations of ball bearings (computer simulation). B JSME 1985; 28: 899-904

[10] Bathe KJ, Finite element procedures in engineering analysis. New Jersey: Prentice-Hall; 1982.

[11] Harris TA, Kotzalas MN. Essential concepts of bearing technology, Rolling bearing analysis. 5th Edition, New York : John Wiley and Sons; 2007.

[12] Sopanen J, Mikola A. Dynamic model of a deep-groove ball bearing including localized and distributed defects. Part 1: theory. P I Mech Eng K-J MBD 2003; 217:201–211.

[13] Anishchenko VS, Astakhov V, Neiman A, Vadivasova T, Schimansky-Geier L. Nonlinear Dynamics of Chaotic and Stochastic Systems, Berlin: Springer; 2007

[14] Ocak H, Loparo KA. Estimation of the running speed and bearing defect frequencies of an induction motor from vibration data. J Mech Syst Signal Pr 2004; 18:515–533.

[15] Abbasion S, Rafsanjani A, Farshidianfar A, Irani N. Rolling element bearings multi-fault classification based on the wavelet denoising and support vector machine. J Mech Syst Signal Pr 2007; 21:2933–2945

**Appendix A**

For a bearing with a stationary outer race, the defect frequencies are given by the following expressions [23]:

The rotational speed of the cage

$$\omega_c = \frac{\omega}{2}\left(1-\frac{d}{D}\cos\alpha\right) \tag{A.1}$$

The outer race defect frequency,

$$\omega_{bpo} = Z\omega_c = \frac{Z\omega}{2}\left(1-\frac{d}{D}\cos\alpha\right) \tag{A.2}$$

The inner race defect frequency,

$$\omega_{bpi} = Z(\omega-\omega_c) = \frac{Z\omega}{2}\left(1+\frac{d}{D}\cos\alpha\right) \tag{A.3}$$

The ball spinning frequency,

$$\omega_b = \frac{\omega}{2}\left(\frac{D}{d}-\frac{d}{D}\cos^2\alpha\right) \tag{A.4}$$

**Appendix B**

The elements of matrix **A** can be calculated as

$$\mathbf{A} = \begin{bmatrix} 0 & 0 & 1 & 0 \\ 0 & 0 & 0 & 1 \\ A_{xx} & A_{xy} & -c/m & 0 \\ A_{yx} & A_{yy} & 0 & -c/m \end{bmatrix} \tag{B.1}$$

Where

$$A_{xx} = -\frac{1}{m}\frac{\partial f_x}{\partial x} = -\frac{3K}{2m}\sum_{j=1}^{Z}\gamma_j\delta_j^{1/2}\cos^2\theta_j \tag{B.2}$$

$$A_{xy} = A_{yx} = -\frac{1}{m}\frac{\partial f_x}{\partial y} = -\frac{1}{m}\frac{\partial f_y}{\partial x} = -\frac{3K}{2m}\sum_{j=1}^{Z}\gamma_j\delta_j^{1/2}\cos\theta_j\sin\theta_j \tag{B.3}$$

$$A_{yy} = -\frac{1}{m}\frac{\partial f_y}{\partial y} = -\frac{3K}{2m}\sum_{j=1}^{Z}\gamma_j\delta_j^{1/2}\sin^2\theta_j \tag{B.4}$$